IEEE Access
Multidisciplinary | Rapid Review | Open Access Journal

Received 12 September 2023, accepted 16 September 2023, date of publication 20 September 2023,
date of current version 27 September 2023.

Digital Object Identifier 10.1109/ACCESS.2023.3317697

RESEARCH ARTICLE

Design and Fabrication of a Minimally Invasive Dielectric Sensor for Biological Environments

I. MARASCO[1], (Member, IEEE), G. NIRO[1], F. RIZZI[2], A. D'ORAZIO[1], (Member, IEEE), M. GRANDE[1], (Member, IEEE), AND M. DE VITTORIO[2,3], (Senior Member, IEEE)

[1]Dipartimento di Ingegneria Elettrica e dell'Informazione, Politecnico di Bari, 70126 Bari, Italy
[2]Center for Biomolecular Nanotechnologies, Istituto Italiano di Tecnologia (IIT), 73010 Arnesano, Italy
[3]Dipartimento di Ingegneria dell'Innovazione, Università del Salento, 73047 Lecce, Italy

Corresponding author: I. Marasco (ilaria.marasco@poliba.it)

ABSTRACT In this paper, a minimally invasive dielectric sensor with a compact footprint of 24×18 mm^2 is presented. It is based on two complementary split ring resonators (CSRRs) fed by a microstrip with coplanar waveguide configuration and placed on a 200 μm thick Kapton substrate. The device has been fabricated by means of a multi-material 3D printer NanoDimension's Dragonfly IV and is characterized by exploiting two different sensing methodologies. As a first step, the device has been characterized in the air by measuring the volume of deionized water droplets placed on one of the CSRRs in the range between 3.6 μl and 9.6 μl. This study has been performed through the analysis of the resonant frequency shift caused by the variation of the dielectric constant. The results show a Q-factor of 702 and a sensitivity of 0.3% μl^{-1}. Then, an additional step has been carried out for the measurement of the temperature of the water in which the sensor is totally dipped. We analyzed the frequency shift due to the water temperature variation in the range between 20°C and 40°C which corresponds to a variation in relative permittivity. In this case, the sensor shows remarkable results in terms of Q-factor, equal to 501, and a sensitivity to dielectric variations in out-of-body and in-body temperature ranges equal to 0.5% and 1.5%, respectively.

INDEX TERMS 3D printing, complementary split ring resonator, dipped sensor, finite difference time domain, flexible complementary split ring resonator, flexible sensor, ingestible sensor, kapton, radio frequency identification, sensor, wearable sensor.

I. INTRODUCTION

Flexible sensors offer big opportunities for the development of non-invasive systems for healthcare applications on the human body [1]. Indeed, the possibility to adapt their shape to curve surfaces together with the higher robustness to external strains make these sensors the most suitable choice for wearable, implantable, and ingestible applications [2], [3], [4], [5], [6], [7], [8], [9], [10]. The literature contains a huge number of sensors based on thin and stretchable substrates [11], [12], [13], [14], [15], [16]. In this context, wireless communication is of paramount importance in order to avoid cables and connectors, [6], [17]. To face this challenge, radio frequency identification (RFID) technology comes to the aid [18], [19]. An RFID system is composed of sensing elements (the tags) and a reader. The reader sends an interrogation signal to the tag whose response is dependent on the measurement conditions. An RFID sensor with optimal performance is characterized by a very high sensitivity and, as a consequence, the effects of material and liquids under test become more intelligible. In the quest for microwave devices sensing the dielectric properties of materials and liquids, a commonly adopted methodology is the analysis of dielectric variations. The dielectric constant varies according to a huge number of parameters such as temperature, humidity, and so on. The sensitivity of dielectric sensors is defined as the ratio between the frequency shift of the device's resonant frequency and the variation of the relative permittivity due to the presence of materials/liquids under test. To be applicable in biological environments, sensors need high robustness against water presence. For example, to function optimally on the skin, sensors need to deal with the formation of drops on their

The associate editor coordinating the review of this manuscript and approving it for publication was Giorgio Montisci.

surface, while for operations inside the body, sensors have to work optimally when fully inserted in tissues, mostly composed of water. Reference [20] details the development of a low-cost flexible RFID humidity sensor. The reported value of its sensitivity is very low, about 0.18%. Another issue can be the absence of standard bands reserved in the working range of the device (7 GHz) which can complicate its integration in RFID systems. In addition, at this frequency, the power consumption is high, and it results more difficult to extrapolate the response of the tag using the backscattering approach. Reference [21] details a flexible RFID sensor for the analysis of the water. Although the very promising results the sensor needs circuitry for the reading, and it is not suitable for wearables.

Among other alternatives, Complementary Split Ring Resonators (CSRRs) offer an optimal trade-off between performance, footprints, and costs [22], [23], [24], [25]. Their integration with RFID protocols can open the door to a new generation of high-sensitive RFID sensors. Reference [26] details a flexible chipless RFID tag based on CSRRs; however, the footprint is large (almost 50 $\times$ 50 mm^2 at 1 GHz). Moreover, the tolerances in the fabrication process have introduced uncertainty in the response of the devices. In addition, the Q-factors and the sensitivities of the sensor have not been detailed and the operation in contact with fluids has not been proven.

In general, the low sensitivities of CSRRs when in contact with fluids, related to low Q-factors, are an extremely important issue to solve. Reference [27] details a CSRR applied for the analysis of fluids, but the Q-factor of the device has a very low value equal to 35. In [28], a device having a higher Q-factor has been designed by combining two resonators which have taken to a sensitivity of 0.87%. In [29] a sensor reporting an even higher sensitivity is detailed. The sensor is implemented using a CSRR on the ground plane of a microstrip and the exposure of the device to the Liquid Under Test (LUT) is obtained using a Poly-DiMethylSiloxane (PDMS) coil-shape microfluidic channel. The use of microfluidics maximizes the effect of LUT on the resonator and leads to a value of sensitivity (0.98%). The contact between the LUT and the resonator is extremely difficult to control. In this sense, submersible sensors are an optimal solution to overcome this challenge. Reference [30] details on a submersible sensor fabricated using two CSRRs (Multiple CSRR, M-CSRRs). However, the sensor has only been tested in oils and presents a Q-factor after the dipping in fluids, very low as the magnitude of the S_{11} dip magnitude becomes lower than 10 dB.

Besides the development of water submersible high-sensitive sensors, the design of flexible CSRR having optimal sensing characteristics is still a challenge to overcome. Planar geometries help the fabrication processes on flexible substrates. Indeed, this configuration leads to two advantages; firstly the patterning of a single metallic layer is needed, therefore alignments are not necessary. Secondly, grounded microstrips imply thicker stacks and ground metallic bottom layers reducing the flexibility of the substrate [31]. A flexible planar CSRR on a 125 μm-thick polyethylene naphthalate is proposed in [32]. However, the device reports a very low Q-factor of 35.1 and it has not been applied for fluid analysis. Reference [33] details a sensor formed of a ring resonator coupled with a coplanar microstrip line. However, the position of the liquid needs to be carefully controlled. In addition, the device is not flexible and presents a large footprint of 40 $\times$ 8 mm^2.

In this paper, we propose an innovative dielectric sensor based on two CSRRs fed by a coplanar microstrip line placed on a 200 μm-thick Kapton substrate which can be exploited for the development of a sensing platform composed of two main blocks, an antenna, and the sensor itself. The sensor presents a twofold sensing methodology coming from the analysis of dielectric variations at two different frequency ranges. For the first methodology, the analysis has been focused on the evaluation of the sensitivity of the device when different volumes of water droplets have been placed on its surface. The working frequency for this study is around 4.6 GHz, (suitable for Internet of things [34] sub-6GHz band of 5G [35], [36] and RFID [19], [37]). The idea behind this choice regards the advantages of using the RFID technology for future applications of the proposed sensor. Indeed, RFID presents some important advantages in the quest for minimally invasive sensors for biological environments such as (i) non-intrusive and real-time monitoring, (ii) data accuracy and precision, and (iii) cost-effectiveness. The sensitivity to water volume is defined as the ratio between the frequency shift of the device's resonant frequency and the variation of the relative permittivity due to the presence of water droplets on the surface. In the proposed analysis the sensitivity is equal to 0.33% μl^{-1} and the Q-factor is equal to 702. For the second methodology, the study has been focused on the measurement of the water temperature when the sensor is totally dipped in it: the aim is to measure the water temperature by analyzing the shift of the working frequency. In this situation, the sensor resonates at around 840 MHz because of the higher dielectric constant of the water (in the range between 72 and 80) with respect to that of the air (equal to 1). Finally, the device reports one of the highest Q-factors in liquids (501) and a sensitivity to dielectric variations in out-of-body and in-body temperature ranges equal to 0.5% and 1.5%, respectively. The performance of the proposed device will be compared with the state of the art in Table 2. The device has been fabricated using a multi-material 3D printer NanoDimension's Dragonfly System. The use of a 3D printer has taken to a very precise fabrication process with a minimum shift between simulations and measurements. Moreover, the process is characterized by the high repeatability of the devices and by a very big yield of 9 resonators printed in less than 2 hours. The feature of being minimally invasive combined with a very compact footprint of 24 $\times$ 18 mm^2 (0.06 λ $\times$ 0.05 λ and 0.375 λ $\times$ 0.28 λ,

where λ is the electrical wavelength at the frequency of 850 MHz and 4.7 GHz, respectively) makes this device an optimal choice for biological environments.

II. DESIGN OF THE RESONATOR

Fig. 1(a) sketches the geometry of the sensor. The device is characterized by a coplanar waveguide (CPW) configuration with two CSRRs working in parallel.

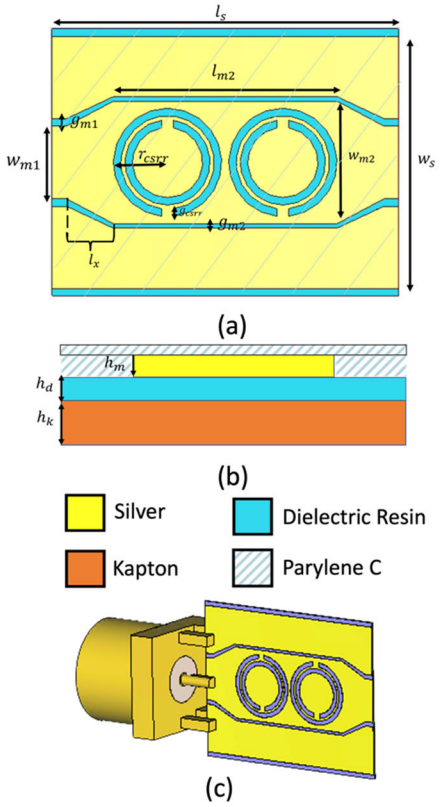

FIGURE 1. Geometry of the sensor: (a) top view with respective geometrical parameters, (b) front view with geometrical parameters, and c) simulation layout.

Each CSRR behaves like an LC resonant circuit [38], [39], and it is characterized by a resonant frequency equal to (1)

$$f_r = \frac{1}{2\pi\sqrt{L_0 C_c}} \tag{1}$$

where L_0 and C_C are the inductance and capacitance of the resonator, respectively. Since its CPWs configuration, it is necessary to properly design the lateral dimensions to achieve a matched line and the central strip can be made wide enough to provide the required space to etch the CSRRs on it. With this approach, the ground plane can be preserved from being etched, and the fabrication step results very fast. After the design of the first CSRR, the second one has been designed in the same way to enhance the Q-factor. The width of the microstrips (w_{m1}, w_{m2}), are constrained by the footprint of the connector and the diameter of the CSRRs respectively, while the gaps g_{m1} and g_{m2} have been designed to achieve an input impedance of 50 Ω. The distance between the two CSRRs has been optimized to enhance the Q-factor of the device and it is equal to 0.5 mm. Since the presence of two CSRRs, the electromagnetic signal traveling into the microstrip is trapped by the resonators, therefore the signals having these frequencies are not reflected on the open circuit at the end of the coplanar waveguide. As a consequence, the S_{11} trend is characterized by a notch frequency for that value.

Fig. 1(b) sketches the vertical cross-section. The substrate is a 200μm-thick Kapton (h_k) with a dielectric constant of 3.8 and a loss tangent equal to 0.002. On the top of the flexible substrate, there is a thin dielectric adhesion layer with a thickness equal to h_d having a dielectric constant of 2.9 and loss tangent of 0.002, and a metallic layer of 35 μm (h_m). The corresponding values of the geometrical parameters are detailed in Table 1.

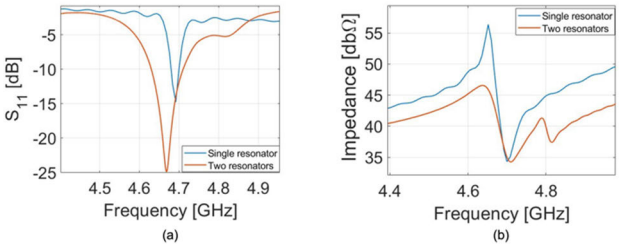

FIGURE 2. Comparison between simulations of the device composed of one resonator (blue curve) and two resonators (red curve) in the air: (a) scattering parameter S_{11}, (b) impedance.

As a first step, the response of the sensor has been simulated in the air by solving the Maxwell equations in the time domain through a Finite Difference Time Domain (FDTD)-based commercial software CST Microwave Studio. In addition, the 3D model of the SMA connector has been placed in the feeding point (Fig. 1c)).

Fig. 2 shows the comparison between the response of the device composed of one resonator (blue curve) and two resonators (red curve) when in air, in terms of scattering parameter S_{11} and impedance. As it can be noted the device composed of two resonators works properly at a frequency of 4.64 GHz with a dip of the magnitude of about 30 dB.

It is worth stressing that the Q-factor in the case of two CSRRs is equal to 940, a significantly higher value with respect to the single one which presents a Q-factor of 280, at the resonant frequency. The evaluation of the Q-factor has been carried out by exploiting the 3dB method from the scattering parameter [40]. The choice to consider two resonators working in parallel represents a trade-off between the sensitivity of the sensor, given by the Q-factor, and the sizes of the footprint compatible with a minimally invasive sensor.

After the analysis in air, a surrounding medium has been introduced in the simulations with relative permittivity and tangent loss equal to that of the deionized water at different temperatures in the range 20°C - 40°C.

The dielectric constant of the water has been varied using (2), where T represents the temperature in °C [41]:

$$\varepsilon_r(T) = 78 \cdot (1 - 0.00461 \cdot (T - 25) + 0.0000155 \cdot (T - 25)^2) \quad (2)$$

The scattering parameter S_{11} has been evaluated in the temperatures under test (24°C−45°C) and as result, the trend of the resonant position (f_r) versus the value of the dielectric constant (ε_r) is reported in Fig. 3. The relative permittivity of the pure water is directly proportional to its temperature; moreover, the resonant frequency of the device increases with the relative permittivity of the pure water in which the sensor is dipped. As a consequence, as can be noted from (2), the higher the temperature the higher the working frequency of the resonator. The resonant position of the sensor is always contained in the 800 MHz band and the simulated values have been interpolated using a polynomial function of degree one having expression in (3).

$$f_r = 1.2224 - 0.0046\epsilon_r \quad (3)$$

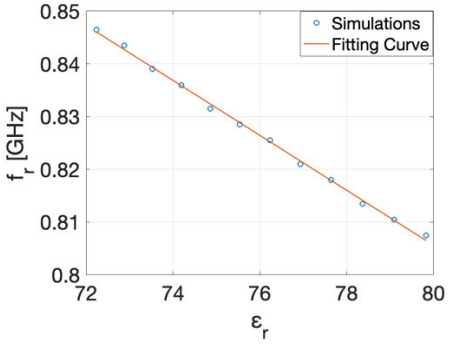

FIGURE 3. Simulation of the device dipped in deionized water: resonant frequency versus dielectric constant.

TABLE 1. Geometrical parameters of the sensor.

Parameter	Value [mm]
w_{m1}	5.00
w_s	0.75
l_s	23.70
g_{m1}	0.50
g_{m2}	0.30
w_{m2}	8.40
l_{m2}	15.30
r_{csrr}	3.70
g_{csrr}	0.3
l_x	7.40
h_m	0.035
h_d	0.003
h_k	0.20

The sensitivity of the sensor (S) has been evaluated as re-ported in (4).

$$S = \frac{df_r}{d\varepsilon_r}\frac{1}{f_0}100 = \frac{0.046}{0.8}100 = 0.56\% \quad (4)$$

III. FABRICATION AND CHARACTERIZATION

The device has been fabricated by means of a multi-material 3D printer, NanoDimension's Dragonfly IV directly on a 200 μm-thick Kapton substrate. 35 μm of silver-based ink (AgCite) have been deposited by hundreds of nozzles at a temperature of 140 °C, necessary to ensure proper atomization of the ink and to guarantee an electrical conductivity of about 2 * 10^7 S/m. The adhesion between the Kapton and the metal has been strengthened by depositing a very thin layer of less than 3 μm of a proprietary dielectric ink (DI 1092), characterized by a relative permittivity equal to 2.3, as for the Kapton. This procedure enables very precise and accurate designs and because of its parallel processing characteristic, this technique shows a high process yield. In addition, the entire process is controlled by the user via a simple interface and does not need to be performed in a clean room to avoid contamination [42]. After the printing process, the device was cut, connectorized, and passivated with 1.02 grams of Parylene C, deposited using room-temperature chemical vapor deposition (CVD) (corresponding to a layer of a thickness of 1 μm).

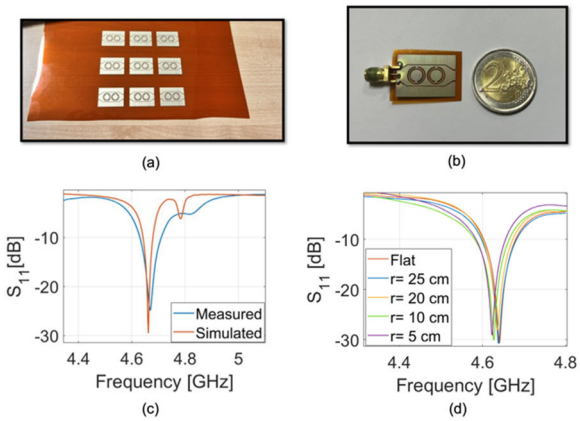

FIGURE 4. Fabrication and characterization- (a) Result of the printing process (b) Proposed resonator, (c) comparison between the simulated and measured S_{11}, (d) measured scattering parameter S_{11} of the device under different bent conditions.

This last step is necessary before the test with water since it makes the surface of the CSRR hydrophobic. The printed sheet containing 9 devices, and the obtained sensor, are shown in Fig. 4(a) and 4(b), respectively. The resonators have been characterized in terms of scattering parameter S_{11} using a Vector Network Analyser (VNA, Anritsu MS432B) and an SMA rigid cable. Fig. 4(c) compares the measured S_{11} with the simulated values. The sensor works properly at the frequency of 4.66 GHz and presents a dip of the S_{11} scattering parameter of about −25 dB. As it can be noted there is an optimal agreement with the simulated model with a minimum shift of a few megahertz due to fabrication tolerances. It is possible to also note a lower S_{11} dip in the measurements, due to the effect of the soldering. The sensor has been tested in bent condition on polystyrene cylinders having radii of curvature compatible with different parts of the human body, equal

to 5, 10, 20, and 25 cm. As it is possible to note from Fig. 4(d), the trend of scattering parameter S_{11} is characterized by a shift of a few MHz with respect to the flat one, in case of bending radius equals to 5 cm and 10 cm.

IV. ANALYSIS OF THE SENSITIVITY

The device has been developed to work in different environments and, to prove the effectiveness of this approach, the sensitivity of the sensor has been tested in both two cases, where in the air the sensitivity to water droplets has been analyzed, while in water, the influence of the temperature on the frequency response has been exploited.

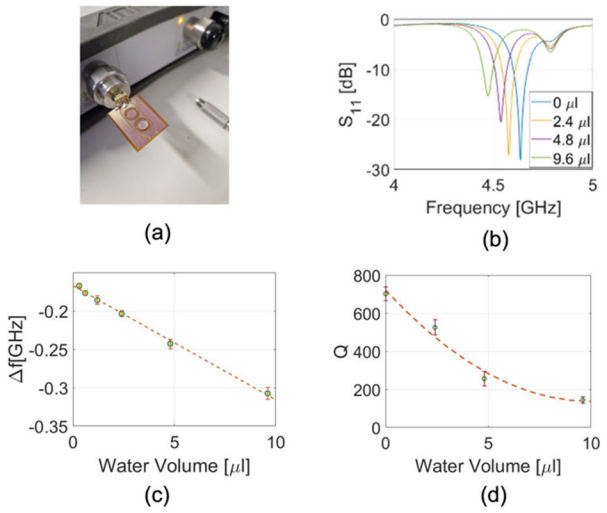

FIGURE 5. Sensitivity of the sensor to water droplets: (a) Sensor connected to the VNA, (b) Scattering parameters S_{11} of the device for various volumes of water droplets, (c) Frequency vs volume of water droplets, (d) Q-Factor vs volume of water droplets.

A. IN AIR SENSITIVITY

When attached to the skin, the sensor is constantly exposed to sweat droplets which influence the frequency response and can be analyzed to extract important information. The sensitivity of the sensor to the water droplets has been tested by measuring the scattering parameter S_{11} after the deposition of volumes of deionized water ranging from 0.3 μl to 9.6 μl. The results are reported in Fig. 5. The sensor has been connected to a VNA in a self-standing configuration as shown in Fig. 5(a). In order to avoid frequency variations due to the position of the drops on the resonator, the analysis has been performed by fixing their position at the center of the one of CSRR (the right one in Fig. 5(a)) using a micropipette and welding loupe. It is worth mentioning that a possible future approach which could be implemented in the case of on-skin analysis, regards the use of microfluidic channels made with hydrophobic/hydrophilic interfaces for the sensitive central zone [43]. As it can be seen from Fig. 5(b) the sensor shows two resonant dips, one at 4.7 GHz, and a second varying with the amount of water placed on the first CSRR leaving the other resonator (the left one in Fig. 5(a)) unexposed to exploit the sensor in differential mode. It can be noted that the higher the water volume, the higher the distance between the dips, and the lower the Q-factor of the first dip. The trend of the distance between the resonant dips versus the volume of deionized water is reported in Fig. 5(c). It is worth stressing that the relationship between the water volume and the differential frequency is linear. The experimental points have been interpolated using a fit curve having the expression in (5)

$$\Delta f(V) = 0 - 0.16718 - 0.014861 \cdot V \tag{5}$$

where Δf (V) is the distance between the resonant dips and V is the volume of the water in microliters. From (5) the sensitivity of the sensor has been evaluated as in (6) reporting a value of 0.3% μl^{-1}

$$S(t) = \frac{d(\Delta f(t))}{dV}\frac{1}{f_0}100 \tag{6}$$

where f_0 is the resonant position of the second dip.

As can be observed from Fig. 5(d), there is an inverse relationship between the Q-factor and the sizes of the water droplets because of an increase in the dielectric losses. The relation between Q and the water volume has been evaluated using a fitting curve having the expression reported in (7).

$$Q(V) = 721.3124 - 116.877V + 5.8434V^2 \tag{7}$$

Further analysis has been carried out in order to emulate the presence of sweat droplets on the CSRR surface. A volume of 9.6 μl with a NaCl concentration in the range of 1%-2% has been considered for the study [44]. The comparison between simulations and measurements has been reported in Fig. 6. It is possible to see that there is a very good agreement between them without any shift of resonant frequency, equal to 4.47 GHz. The reason behind these results is the very small amount of NaCl considered in a small volume of water.

B. IN WATER SENSITIVITY

The human body is made up of 60% water, therefore it is extremely important for an ingestible sensor to work properly when totally dipped. The characterization in deionized water has been performed by dipping the sensor in a PET container, large enough to avoid effects on the measurements due to its

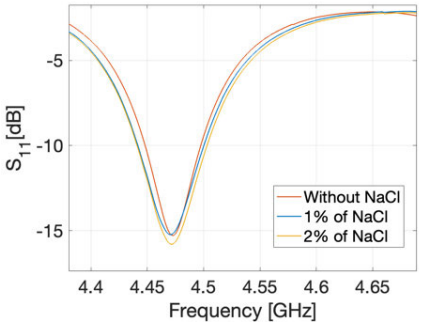

FIGURE 6. Scattering parameter S_{11} at different concentrations of NaCl in a volume of 9.6 μl of deionized water.

walls. Below the container, a hot plate (IKA C-MAG HP 4) set at a fixed temperature of 100°C has been placed. The temperature has been recorded periodically with a digital thermometer (TFA Dostmann LT-102), whose probe has been placed at around 4 cm (Fig.7a)). The analysis of scattering parameter S_{11} has been performed in the range of temperature between 20°C and 40°C.

In Fig. 7(b) the comparison between the measured and simulated scattering parameter S_{11} of the device when dipped in the water at 35°C is reported. The simulated water is characterized by a relative permittivity derived from (2) and a loss tangent reported in [45]. It is possible to note that there is a very good agreement between simulation and measurements with only a shift of 2 MHz: the measured scattering parameter S_{11} shows a dip of −20 dB at 828 MHz (blue curve), while the simulated one presents at 826 MHz a dip of −19.7 dB (red curve). Fig. 7(c) illustrates the scattering parameter S_{11} taken at various water temperatures; an increase in the resonant frequency with the temperature can be observed. It is worth stressing that increasing the temperature reduces the dielectric losses of the water sharpening the dips of the S_{11} and increasing the Q-factor of the resonator.

The sensitivity of the sensor has been evaluated in all the temperature ranges to analyze the influence of the Q-factor on the response of the device using (8), (9), (10):

$$\Delta = \frac{\Delta f\,(T)}{f_0}\frac{1}{\Delta\varepsilon_r(T)}100 \tag{8}$$

$$\Delta f\,(t) = f_r\,(T) - f_0 \tag{9}$$

$$\Delta\varepsilon_r = \varepsilon_r\,(T) - \varepsilon_r(20^\circ C) \tag{10}$$

where f_o is the resonant frequency when the water temperature (T) is at 20°C, and the variation of the dielectric constant at the different water temperatures (ε_r (T)) has been evaluated using (2). The trend of Δ and Q concerning the temperature have been compared in Fig. 7(d). From Fig. 7(c) and 7(d), the water temperature variation has two effects on the response of the device: the variation of the resonant frequency and of the sensitivity. So, it results that the relation between temperature and working frequency cannot be considered linear in all the ranges between 20°C and 40°C. For these reasons, the experimental data (frequency vs temperature) have been subdivided into two linear sets: below and above 35°C. Then, two expressions have been extrapolated for the calibration curves reported in (11) and (12).

$$f\,(T) = 0.8 + 1.4 * 10^{-3}T, \quad T \in [20^\circ C, 35^\circ C] \tag{11}$$

$$f\,(T) = 0.823 + 5 * 10^{-3}T, \quad T \in [35^\circ C, 40^\circ C] \tag{12}$$

As can be noted from Fig. 8(a), the out-of-the-body temperature range has a slope of 1.4 * 10^{-3} GHz°C^{-1} and a sensitivity to dielectric constant variation equal to 0.5%; while the sensor in the body temperature range (Fig. 8(b)) has a higher slope of 5 * 10^{-3} GHz GHz°C^{-1}, with the corresponding sensitivity of 1.5% if referred to as dielectric variations.

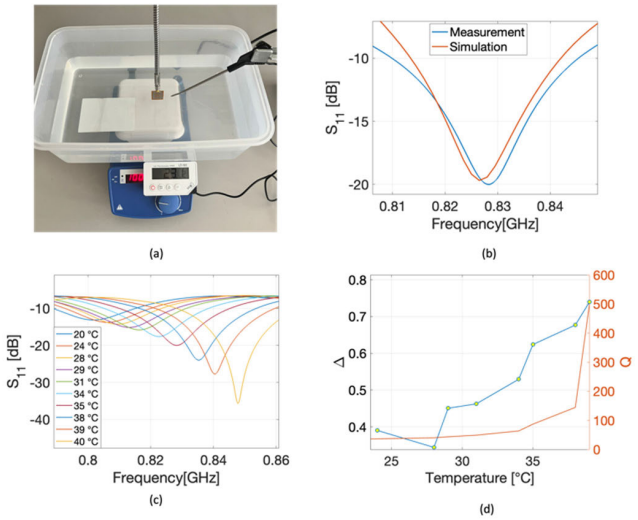

FIGURE 7. (a) Measurements setup, (b) Comparison between simulation and measurements at 35° (c) S_{11} for various temperatures, (d) Sensitivity and Q-factor vs temperature variations.

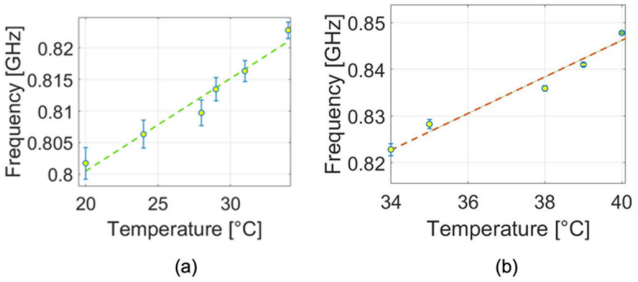

FIGURE 8. Calibration curves: (a) Lower-sensitive region outside the body, (b) higher-sensitive region inside the body-temperature region.

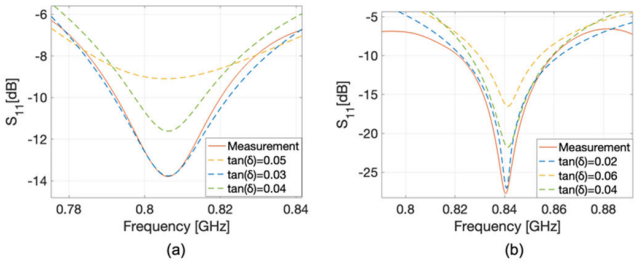

FIGURE 9. Parametrical sweep of the tangent loss of the deionized water at (a) 25°C and (b) 40°C.

A further analysis has been carried out in order to estimate the losses of the water at temperatures equal to 25° and 40 °C. A parametric sweep for tangent loss has been performed in order to verify the good agreement between simulations and measurements. As reported in Fig. 9, the agreement has been obtained for tag(δ) = 0.03 at 25°C (Fig. 9(a)) and for tag(δ) = 0.02 at 40 °C (Fig. 9(b)). The obtained values are in line with those reported in [45].

Finally, the performances of the sensor have been compared with the state of the art in Table 2. As it is possible to observe the footprint is about eight times smaller than the others if compared with electrical lengths. Moreover, this

sensor is the only one suitable for RFID applications as works in the 800 MHz band with the highest Q-factor and the best sensitivity in liquid environments. Finally, this sensor is the only flexible and is characterized by a planar geometry, very lightweight and straightforward to be produced in roll-2-roll processes.

TABLE 2. Comparison of the proposal with the state-of-the-art.

	[32]	[30]	[29]	T.W.
Footprint [mm^2]	40x8	15x25	35x20	24x18
Frequency [GHz]	2.6	7.6	2.26	0.8
Submersible	No	Yes	No	Yes
Q-factor (air)	42	937	N.D.	702
Q-factor (s.sed)	-	-	-	600
Diel. Sensitivity [%]	0.27	-	0.98	1.5
Drop. Sensitivity [% µl^{-1}]	-	-	-	0.3
Temp. Sensitivity [% C^{-1}]	-	-	-	0.5
Planar	Yes	No	No	Yes
Flexible	No	No	No	Yes

V. CONCLUSION

Low-invasive microwave sensors offer big advantages for classical bulk and low-frequency technologies. The use of flexible materials allows the devices to adapt their shape to curve surfaces as the human body enhances wearability. Moreover, with the use of microwave frequencies cables and connectors can be avoided minimizing the impact of the sensors. In this scenario, the design and fabrication of sensors able to operate in water take interesting new perspectives, especially in sweat monitoring or edible sensors. In this paper, a CSRR-based sensor on a flexible Kapton substrate has been proposed. The device has been fabricated using a 3D multi-material 3D printer and coated with Parylene C. The obtained process yield is high as 9 resonators have been obtained in less than 2 hours. The device presents optimal performance with very high Q-factors of 702 and 501 when in air and in water, respectively, proving its suitability in healthcare applications. This is also demonstrated since the sensor presents an identical behavior on different bent conditions. High sensitivity to water droplets when in the air has been proven suggesting its use in wearable sweat or humidity sensors. Then the sensitivity versus temperature in water has been tested, reporting optimal performances that overcome the state of the art in terms of footprint, sensitivity, and Q-factor. In addition, a further analysis has been performed to estimate the losses of the water at two temperatures equal to 25°C and 40°C. Moreover, the integration of the sensor with external antennas can pave the way for the development of a passive and wireless water temperature sensing platform [17], [46]. Future developments regard the test of the sensor out of the water, against other agents such as pH or external strains and in the water under bending conditions. Finally, the use of a multi-material 3D printer allows the fabrication of dielectric containers, microfluidic channels, or needles. This approach can reduce drastically the times for prototyping high-sensitive sensors on flexible substrates.

ACKNOWLEDGMENT

(M. Grande and M. De Vittorio are co-first authors.)

REFERENCES

[1] Z. Wang, L. Sun, Y. Ni, L. Liu, and W. Xu, "Flexible electronics and healthcare applications," *Frontiers Nanotechnol.*, vol. 3, pp. 1–10, Mar. 2021, doi: 10.3389/fnano.2021.625989.

[2] C. Loss, R. Gonçalves, C. Lopes, P. Pinho, and R. Salvado, "Smart coat with a fully-embedded textile antenna for IoT applications," *Sensors*, vol. 16, no. 6, p. 938, Jun. 2016, doi: 10.3390/s16060938.

[3] S. Kanaparthi, V. R. Sekhar, and S. Badhulika, "Flexible, eco-friendly and highly sensitive paper antenna based electromechanical sensor for wireless human motion detection and structural health monitoring," *Extreme Mech. Lett.*, vol. 9, pp. 324–330, Dec. 2016, doi: 10.1016/j.eml.2016.09.007.

[4] X. Yang and M. Zhang, "Review of flexible microelectromechanical system sensors and devices," *Nanotechnol. Precis. Eng.*, vol. 4, no. 2, Jun. 2021, Art. no. 025001, doi: 10.1063/10.0004301.

[5] I. Marasco, G. Niro, L. Lamanna, L. Piro, F. Guido, L. Algieri, V. M. Mastronardi, A. Qualtieri, E. Scarpa, D. Desmaële, F. Rizzi, A. D'Orazio, M. De Vittorio, and M. Grande, "Compact and flexible meander antenna for surface acoustic wave sensors," *Microelectron. Eng.*, vol. 227, Apr. 2020, Art. no. 111322, doi: 10.1016/j.mee.2020.111322.

[6] Z. Xie, R. Avila, Y. Huang, and J. A. Rogers, "Flexible and stretchable antennas for biointegrated electronics," *Adv. Mater.*, vol. 32, no. 15, Apr. 2020, Art. no. 1902767, doi: 10.1002/adma.201902767.

[7] Y. Khan, A. Thielens, S. Muin, J. Ting, C. Baumbauer, and A. C. Arias, "A new frontier of printed electronics: Flexible hybrid electronics," *Adv. Mater.*, vol. 32, no. 15, Apr. 2020, Art. no. 1905279, doi: 10.1002/adma.201905279.

[8] P. Wang, M. Hu, H. Wang, Z. Chen, Y. Feng, J. Wang, W. Ling, and Y. Huang, "The evolution of flexible electronics: From nature, beyond nature, and to nature," *Adv. Sci.*, vol. 7, no. 20, Oct. 2020, Art. no. 2001116, doi: 10.1002/advs.202001116.

[9] J. Yang, S. Luo, X. Zhou, J. Li, J. Fu, W. Yang, and D. Wei, "Flexible, tunable, and ultrasensitive capacitive pressure sensor with microconformal graphene electrodes," *ACS Appl. Mater. Interface*, vol. 11, no. 16, pp. 14997–15006, Apr. 2019, doi: 10.1021/acsami.9b02049.

[10] H. Zhang, Y. Lan, S. Qiu, S. Min, H. Jang, J. Park, S. Gong, and Z. Ma, "Flexible and stretchable microwave electronics: Past, present, and future perspective," *Adv. Mater. Technol.*, vol. 6, no. 1, pp. 1–12, Jan. 2021, doi: 10.1002/admt.202000759.

[11] P. Wang, W. Yu, G. Li, C. Meng, and S. Guo, "Printable, flexible, breathable and sweatproof bifunctional sensors based on an all-nanofiber platform for fully decoupled pressure–temperature sensing application," *Chem. Eng. J.*, vol. 452, Jan. 2023, Art. no. 139174, doi: 10.1016/j.cej.2022.139174.

[12] C. Dagdeviren, F. Javid, P. Joe, T. von Erlach, T. Bensel, Z. Wei, S. Saxton, C. Cleveland, L. Booth, S. McDonnell, J. Collins, A. Hayward, R. Langer, and G. Traverso, "Flexible piezoelectric devices for gastrointestinal motility sensing," *Nature Biomed. Eng.*, vol. 1, no. 10, pp. 807–817, Oct. 2017, doi: 10.1038/s41551-017-0140-7.

[13] Y. Fu, S. Zhao, and R. Zhu, "A wearable multifunctional pulse monitor using thermosensation-based flexible sensors," *IEEE Trans. Biomed. Eng.*, vol. 66, no. 5, pp. 1412–1421, May 2019, doi: 10.1109/TBME.2018.2873754.

[14] C. M. Boutry, L. Beker, Y. Kaizawa, C. Vassos, H. Tran, A. C. Hinckley, R. Pfattner, S. Niu, J. Li, J. Claverie, Z. Wang, J. Chang, P. M. Fox, and Z. Bao, "Biodegradable and flexible arterial-pulse sensor for the wireless monitoring of blood flow," *Nature Biomed. Eng.*, vol. 3, no. 1, pp. 47–57, Jan. 2019, doi: 10.1038/s41551-018-0336-5.

[15] S.-F. Tseng and Y.-S. Tsai, "Highly sensitive humidity sensors based on Li-C_3N_4 composites on porous graphene flexible electrodes," *Appl. Surf. Sci.*, vol. 606, Dec. 2022, Art. no. 155001, doi: 10.1016/J.APSUSC.2022.155001.

[16] L. Natta, F. Guido, L. Algieri, V. M. Mastronardi, F. Rizzi, E. Scarpa, A. Qualtieri, M. T. Todaro, V. Sallustio, and M. De Vittorio, "Conformable AlN piezoelectric sensors as a non-invasive approach for swallowing disorder assessment," *ACS Sens.*, vol. 6, no. 5, pp. 1–11, 2021, doi: 10.1021/acssensors.0c02339.

[17] I. Marasco, G. Niro, V. M. Mastronardi, F. Rizzi, A. D'Orazio, M. De Vittorio, and M. Grande, "A compact evolved antenna for 5G communications," *Sci. Rep.*, vol. 12, no. 1, p. 10327, Jun. 2022, doi: 10.1038/s41598-022-14447-9.

[18] H. Landaluce, L. Arjona, A. Perallos, F. Falcone, I. Angulo, and F. Muralter, "A review of IoT sensing applications and challenges using RFID and wireless sensor networks," *Sensors*, vol. 20, no. 9, p. 2495, Apr. 2020, doi: 10.3390/s20092495.
[19] F. Costa, S. Genovesi, M. Borgese, A. Michel, F. A. Dicandia, and G. Manara, "A review of RFID sensors, the new frontier of Internet of Things," *Sensors*, vol. 21, no. 9, p. 3138, Apr. 2021, doi: 10.3390/s21093138.
[20] E. Md. Amin, Md. S. Bhuiyan, N. C. Karmakar, and B. Winther-Jensen, "Development of a low cost printable chipless RFID humidity sensor," *IEEE Sensors J.*, vol. 14, no. 1, pp. 140–149, Jan. 2014, doi: 10.1109/JSEN.2013.2278560.
[21] X. Qian, Z. Li, Z. Meng, N. Gao, and Z. Zhang, "Flexible RFID tag for sensing the total minerals in drinking water via smartphone tapping," *IEEE Sensors J.*, vol. 21, no. 21, pp. 24749–24758, Nov. 2021, doi: 10.1109/JSEN.2021.3113797.
[22] H. Kou, Q. Tan, Y. Wang, G. Zhang, S. Shujing, and J. Xiong, "A microwave SIW sensor loaded with CSRR for wireless pressure detection in high-temperature environments," *J. Phys. D, Appl. Phys.*, vol. 53, no. 8, Feb. 2020, Art. no. 085101, doi: 10.1088/1361-6463/ab58f2.
[23] T. Yun and S. Lim, "High-Q and miniaturized complementary split ring resonator-loaded substrate integrated waveguide microwave sensor for crack detection in metallic materials," *Sens. Actuators A, Phys.*, vol. 214, pp. 25–30, Aug. 2014, doi: 10.1016/j.sna.2014.04.006.
[24] H. Rmili, K. Alkhalifeh, M. Zarouan, W. Zouch, and M. T. Islam, "Numerical analysis of the microwave treatment of palm trees infested with the red palm weevil pest by using a circular array of Vivaldi antennas," *IEEE Access*, vol. 8, pp. 152342–152350, 2020, doi: 10.1109/ACCESS.2020.3017517.
[25] J. G. D. Oliveira, E. N. M. G. Pinto, V. P. S. Neto, and A. G. D'Assunção, "CSRR-based microwave sensor for dielectric materials characterization applied to soil water content determination," *Sensors*, vol. 20, no. 1, p. 255, Jan. 2020, doi: 10.3390/s20010255.
[26] M. E. B. Jalil, M. K. A. Rahim, H. Mohamed, N. A. B. Samsuri, N. A. Murad, R. Dewan, H. B. A. Majid, N. B. M. Nafis, L. O. Nur, and B. S. Nugroho, "High capacity and miniaturized flexible chipless RFID tag using modified complementary split ring resonator," *IEEE Access*, vol. 9, pp. 33929–33943, 2021, doi: 10.1109/ACCESS.2021.3061792.
[27] A. Javed, A. Arif, M. Zubair, M. Q. Mehmood, and K. Riaz, "A low-cost multiple complementary split-ring resonator-based microwave sensor for contactless dielectric characterization of liquids," *IEEE Sensors J.*, vol. 20, no. 19, pp. 11326–11334, Oct. 2020, doi: 10.1109/JSEN.2020.2998004.
[28] A. Buragohain, A. T. T. Mostako, and G. S. Das, "Low-cost CSRR based sensor for determination of dielectric constant of liquid samples," *IEEE Sensors J.*, vol. 21, no. 24, pp. 27450–27457, Dec. 2021, doi: 10.1109/JSEN.2021.3124329.
[29] L.-C. Fan, W.-S. Zhao, D.-W. Wang, Q. Liu, S. Chen, and G. Wang, "An ultrahigh sensitivity microwave sensor for microfluidic applications," *IEEE Microw. Wireless Compon. Lett.*, vol. 30, no. 12, pp. 1201–1204, Dec. 2020, doi: 10.1109/LMWC.2020.3029060.
[30] X. Zhang, C. Ruan, W. Wang, and Y. Cao, "Submersible high sensitivity microwave sensor for edible oil detection and quality analysis," *IEEE Sensors J.*, vol. 21, no. 12, pp. 13230–13238, Jun. 2021, doi: 10.1109/JSEN.2021.3067933.
[31] J. Muñoz-Enano, P. Vélez, M. Gil, and F. Martín, "Planar microwave resonant sensors: A review and recent developments," *Appl. Sci.*, vol. 10, no. 7, p. 2615, Apr. 2020, doi: 10.3390/app10072615.
[32] Y. M. Wei, X. G. Guo, L. Chen, and Y. M. Zhu, "A novel coplanar waveguide resonator on flexible substrate," *Optik*, vol. 127, no. 20, pp. 9937–9941, Oct. 2016, doi: 10.1016/j.ijleo.2016.07.095.
[33] M. Abdolrazzaghi, M. Daneshmand, and A. K. Iyer, "Strongly enhanced sensitivity in planar microwave sensors based on metamaterial coupling," *IEEE Trans. Microw. Theory Techn.*, vol. 66, no. 4, pp. 1843–1855, Apr. 2018, doi: 10.1109/TMTT.2018.2791942.
[34] L. Atzori, A. Iera, and G. Morabito, "The Internet of Things: A survey," *Comput. Netw.*, vol. 54, no. 15, pp. 2787–2805, Oct. 2010, doi: 10.1016/j.comnet.2010.05.010.
[35] J. G. Andrews, S. Buzzi, W. Choi, S. V. Hanly, A. Lozano, A. C. K. Soong, and J. C. Zhang, "What will 5G be?" *IEEE J. Sel. Areas Commun.*, vol. 32, no. 6, pp. 1065–1082, Jun. 2014, doi: 10.1109/JSAC.2014.2328098.
[36] I. Marasco, G. Niro, F. Rizzi, M. De Vittorio, A. D'Orazio, and M. Grande, "Design of a PEN-based flexible PIFA antenna operating in the sub-6 GHz band for 5G applications," in *Proc. 22nd Int. Conf. Transparent Opt. Netw. (ICTON)*, Jul. 2020, pp. 1–4, doi: 10.1109/ICTON51198.2020.9203160.
[37] I. Bouhassoune, H. Chaibi, A. Chehri, and R. Saadane, "A review of RFID-based Internet of Things in the healthcare area, the new horizon of RFID," *Proc. Comput. Sci.*, vol. 207, pp. 4151–4160, Jan. 2022, doi: 10.1016/j.procs.2022.09.478.
[38] F. Martíín, M. Sorolla, and R. Marqués, *Metamaterials With Negative Parameters: Theory, Design and Microwave Applications*. Hoboken, NJ, USA: Wiley, 2008.
[39] J. D. Baena, J. Bonache, F. Martin, R. M. Sillero, F. Falcone, T. Lopetegi, M. A. G. Laso, J. Garcia-Garcia, I. Gil, M. F. Portillo, and M. Sorolla, "Equivalent-circuit models for split-ring resonators and complementary split-ring resonators coupled to planar transmission lines," *IEEE Trans. Microw. Theory Techn.*, vol. 53, no. 4, pp. 1451–1461, Apr. 2005.
[40] R. S. Kwok and J.-F. Liang, "Characterization of high-Q resonators for microwave filter applications," *IEEE Trans. Microw. Theory Techn.*, vol. 47, no. 1, pp. 111–114, Jan. 1999, doi: 10.1109/22.740093.
[41] T. Meissner and F. J. Wentz, "The complex dielectric constant of pure and sea water from microwave satellite observations," *IEEE Trans. Geosci. Remote Sens.*, vol. 42, no. 9, pp. 1836–1849, Sep. 2004, doi: 10.1109/TGRS.2004.831888.
[42] B. Mohamadzade, R. M. Hashmi, R. B. V. B. Simorangkir, R. Gharaei, S. U. Rehman, and Q. H. Abbasi, "Recent advances in fabrication methods for flexible antennas in wearable devices: State of the art," *Sensors*, vol. 19, no. 10, p. 2312, May 2019, doi: 10.3390/s19102312.
[43] K. Tsougeni, D. Papageorgiou, A. Tserepi, and E. Gogolides, "'Smart' polymeric microfluidics fabricated by plasma processing: Controlled wetting, capillary filling and hydrophobic valving," *Lab Chip*, vol. 10, no. 4, pp. 462–469, 2010, doi: 10.1039/B916566E.
[44] N. D. Pavlov and Y. A. Baloshin, "Electromagnetic properties of liquids at GHz frequencies for medical tasks and metamaterial applications," in *Proc. Days Diffraction (DD)*, May 2015, pp. 1–4, doi: 10.1109/DD.2015.7354866.
[45] A. Andryieuski, S. M. Kuznetsova, S. V. Zhukovsky, Y. S. Kivshar, and A. V. Lavrinenko, "Water: Promising opportunities for tunable all-dielectric electromagnetic metamaterials," *Sci. Rep.*, vol. 5, p. 13535, Aug. 2015, doi: 10.1038/srep13535.
[46] I. Marasco, G. Niro, G. de Marzo, F. Rizzi, A. D'Orazio, M. Grande, and M. De Vittorio, "Design and fabrication of a plastic-free antenna on a sustainable chitosan substrate," *IEEE Electron Device Lett.*, vol. 44, no. 2, pp. 341–344, Feb. 2023, doi: 10.1109/LED.2022.3232986.

I. MARASCO (Member, IEEE) received the master's degree (summa cum laude) in telecommunication engineering from Politecnico di Bari, in October 2019, and the Ph.D. degree, in 2022. Her master's thesis was titled "Flexible Meander Antenna for SAW Sensors." Since November 2019, she has been with the NPEG-Laboratory, as a Ph.D. student in collaboration with Istituo Italiano di Tecnologia (IIT), Arnesano (LE). Since February 2023, she has been an Assistant Professor of electromagnetic fields with Politecnico di Bari. Her main research interests include electrically small antennas on wearable and biodegradable substrates, fabrication technologies for flexible and compact antennas, and piezoelectric resonators for microwave filters and sensors.

G. NIRO received the master's degree in telecommunications engineering from Politecnico di Bari, in 2019, where he is currently pursuing the Ph.D. degree. He is with the Italian Institute of Technology (IIT), Arnesano (LE). His research interests include microwaves resonators, antennas, and piezoelectric sensors.

F. RIZZI received the Ph.D. degree in physics, in 2004. He is currently a Research Staff Member with the Center of Biomolecular Nanotechnologies, Istituto Italiano di Tecnologia, Lecce. He held a postdoctoral training with the Department of Physics, Institute of Photonics, University of Strathclyde, Glasgow, U.K., where he won an Experienced Researcher Marie Curie Fellowship. He has authored more than 70 manuscripts on international journals and proceedings of international conferences, two patents, and three book chapters. His research interests and activities are related on bioinspired micro electromechanical systems design and fabrication for applications in biological and environmental sensing, and artificial hair cells fabrication for flow sensing in robotics.

A. D'ORAZIO (Member, IEEE) received the Laurea degree (summa cum laude) in electrical engineering from the University of Bari, in 1983, and the Ph.D. degree in electromagnetisms, in 1987. She has been an Assistant Professor, since 1990, an Associate Professor, 1998, and a Full Professor of electromagnetic fields with Politecnico di Bari, since 2003. She was the Depute Chancellor of Politecnico di Bari and a member of the Board of Governors, in 2003. Since 2003, she acts as an expert reviewer of projects financed by MIUR, European Commission (VII FP and Horizon 2020), by Apulia region. She was the Coordinator of the Ph.D. course in electronic engineering, from 2004 to 2009. Since 2011, she has been a member of the Management Committee, CNIT. She is a Principal Investigator of research projects funded by MIUR and research contracts funded by national and international companies. She was involved in the COST Actions 268, 288, P11, MP0702, and MP0805. The research concerning the design, fabrication and characterization of microwave and optical devices, antennas, and graphene-based devices is documented by more than 300 publications published on international journals and conference proceedings, and invited papers. She is a member of OSA, AEIT, and SIEm. She is a member of the Management Committee, European COST actions 268 and 288. She was a member of the Executive Board of the ARTI-Regione Puglia. She is a component of scientific committees of national and international conferences.

M. GRANDE (Member, IEEE) received the Laurea degree (summa cum laude) in electronic engineering and the Ph.D. degree from Politecnico di Bari, in 2006 and 2010, respectively. Since October 2015, he has been an Assistant Professor of electromagnetic fields with Politecnico di Bari. His research interests include smart antennas, photonic crystals, plasmonic nanostructures, and graphene-based devices operating in both optical and microwave regimes.

M. DE VITTORIO (Senior Member, IEEE) is currently the Coordinator of the Center for Biomolecular Nanotechnologies, Istituto Italiano di Tecnologia, Lecce, Italy, and a Full Professor with Università del Salento, where he is a Lecturer of the courses ''Electronic and Photonic Devices'' and ''Nanotechnologies for Electronics.'' He has been responsible for more than ten years of the Nanodevice Division, National Nanotechnology Laboratory (NNL), CNR Istituto Nanoscience. During his career, he has designed and coordinated micro and nanofabrication facilities with both backend and frontend technologies, with full prototyping and small/medium scale production capabilities. He has been a consultant for high-tech corporations and a founder/advisor of four startup companies. He is the author of 280 manuscripts on indexed journals, 70 conference proceedings, 14 patents, ten book chapters, and more than 60 invited/keynote talks to international conferences. His research interests include the development of science and technology applied to nanophotonics, nanoelectronics and nano and micro electromechanical systems (NEMS/MEMS) for applications in the fields of life science, and energy and ICT. He is a Senior Editor of the Journal IEEE TRANSACTIONS ON NANOTECHNOLOGY, a Board Member of the International Micro and Nanoengineering Society (iMNEs), and a member of the Editorial Board of the *Journal Microelectronic Engineering*.

Open Access funding provided by 'Politecnico di Bari' within the CRUI CARE Agreement